Assaying neural patterns using scalp electroencephalography from children in a naturally engaging unconstrained video game playing experience

Aryan Mobiny[1,+], Akshay Sujatha Ravindran[1,+], Jesus G Cruz-Garza[1], Andrew Paek[1], Anastasiya Kopteva[1], Sara Eshaghi[1], and José L Contreras Vidal[1,*]

[1]Noninvasive Brain-Machine Interface System Laboratory, Dept. of Electrical and Computer Engineering, University of Houston, Houston, TX, 77004, USA
[*]jlcontreras-vidal@uh.edu
[+]these authors contributed equally to this work

ABSTRACT

Understanding the developing brain in action remains one of the challenges in neuroscience. Developing neural networks are likely to be endowed with functionally important variability across context, age, gender and other, as yet unknown, variables. Thus, it is critical to quantify, describe, and understand the role of naturally occurring neural variability in the developing brain. To examine how neural responses vary across such factors, we assayed neural activity of children at baseline and while they played a videogame at the Children's Museum of Houston. Brain responses and head motion were acquired using mobile brain-body imaging technology. Age effects on spectral content and sample entropy during baseline were consistent with previous developmental studies conducted in laboratory settings. Unsupervised clustering of spectral brain patterns in baseline and task conditions uncovered 'common' and 'rare' patterns selective for age and/or skill level or independent of such factors. A temporal cluster characterized by high beta power was observed predominantly in 10 year-olds and younger children, whereas a frontal cluster characterized by high gamma power was associated with skill level. No gender effects on spectral patterns were found. These findings are the first to quantify and describe brain patterns observed during gameplay in freely behaving children.

Introduction

One of the grand challenges in developmental cognitive-motor neuroscience is to advance understanding of the developing human brain in "action and in context" in complex real settings to study naturally occurring neural variability. Fortunately, recent developments in mobile brain-body imaging (MoBI) technology has facilitated the non-invasive recording and analysis of brain activity and movement with high temporal resolution in naturalistic settings[1–3]. This technology however has yet to significantly reach the pediatric population, which is critical to acquire fundamental knowledge about developing neural activity patterns in children in health and disease[4–7]. Moreover, quantitative EEG (or qEEG) measurements have diagnostic value as objective endpoints for measuring the efficacy of experimental interventions. However, despite their growing importance, very little is known about the constancy and variability of qEEG measurements in the general population and in the pediatric population specifically. Previous studies have reported that many infants who do not possess any neuroimaging abnormalities at birth experienced different neurological disorders later in life[8]. Therefore, characterizing the normative maturation of neural patterns in the developing brain will allow for the timely detection of neurological disorders, as well as a deeper understanding of their development. In this regard, the study conducted by the Committee on Children with Disabilities[9] reported that the early intervention in the diagnosis of diverse neurological diseases, such as autism, yields better long-term outcomes. For example, different qEEG profiles have been acknowledged with children having attention deficit disorder[10,11], and complexity measures such as multiscale entropy have shown abnormal EEG values linked to childhood neurological disorders[12].

In regard to qEEG, longitudinal studies[13] uncovered deviations in the relative and absolute band powers in children as a consequence of brain maturation with age. For young infants (5–24 months) of age, an alpha-like frequency peak emerges at 5-9 Hz at frontal and central locations which is related to the change in motor behavior that peaks in the second year of life[14,15]. For school-age populations, the resting-state EEG exhibits a decreasing trend in low-frequency bands (delta, theta) with respect to age[16],which is usually attributed to brain maturation[13]. All through adolescence, the peak alpha frequency escalates and reaches the adult level of 10 Hz at the age of 10–12 years[17].

Even though these studies have helped us advance our understanding of the human developing brain in general, most of these studies were performed under constrained experimental settings in a laboratory environment. To understand the brain in action and in context, it has become critical to assay the brain activity patterns in natural and engaging conditions, as children modulate behavior in response to the complex and dynamic nature of the natural environment[18]. For instance, performing an attention-requiring task in a natural environment involves ignoring a variety of distractors; organizing the subject's behavior considering the consequences within the complex environment, and adapting to changing environments at home, work or play.

Recent studies have analyzed the brain response during video gameplay to better understand the underlying neural processes involved in this increasingly popular and social activity. Video games (a $30.4 Billion enterprise in 2016) are played by 97% of teenagers (between the ages of 12 and 17) and 72% of the general population as reported by the Entertainment Software Association or ESA[19]. According to a recent report[20], 67% of US households own a gaming device and 65% of them are home to at least one person who plays more than 3 hours a week. Using qEEG, Mathewson and colleagues reported that delta (0.1-4Hz) and alpha (8-12Hz) rhythms during gameplay can predict learning and skill improvements[21]. Moreover, frontal midline theta-wave activity (4-8Hz) is known to increase over time during gameplay compared to a 'resting' control condition[22]. Changes in other frequency bands and scalp location have also been reported during videogame play. In this regard, an attenuation of central mu rhythm (10-13 Hz) has also been observed[23]. In addition, the absolute power in occipital, parietal, frontal and motor regions in the beta band (12-25 Hz) is higher during videogaming compared to one sitting idle[24]. The attention and vigilance led beta rhythms to increase during a gameplay[25]. However, all these studies discussed above were conducted in a laboratory setting and the significance of the findings may be limited by the small sample population tested in those studies.

Video gaming presents an opportunity to assess brain activity in children given these games deliver an interactive environment packed with gaming narratives and incentives (e.g., gaming points, game levels, etc.) that makes it a highly engaging activity in children[26]. This makes video gaming an ideal task to capture the natural interest of the subjects (e.g., user's engagement) without enforcing any outside constraints. Thus, videogames promote the development of emotional, cognitive and behavioral connections between the user and the game resource[27].

Thus, in this study we deployed MoBI technology in a museum setting to examine the brain activity patterns of children playing a videogame (Minecraft). The goals were to: 1) quantify brain responses in children during an engaging task in a stimulating social environment, which may elicit natural responses from children otherwise not observed within a laboratory setting; 2) acquire data from a relatively large number of children with diverse demographic background with the potential of very high scalability; and 3) characterizing the effects of age, gender and skill levels in the brain activity of the participants.

Material and Methods

Participants

Two hundred and thirty three (233) children (167 males/ 66 females) aged 6 to 16 years-old participated in this experiment at the Children's Museum of Houston during a special one-day event. The experimental protocol, Informed Consent form, and the Photo Release form were approved by the University of Houston Institutional Review Board. Potential participants approached the experiment area and requested information about the event and the technology. Potential participants were given a brief overview of the study, how mobile dry EEG works, and the expected goals and methods of data analysis. If participants agreed to participate, they were fitted with an EEG headset. Parents or guardians signed voluntarily an Informed Consent and the Photo Release forms, whereas children were asked to assent to the experiment.

Experimental Procedure and Data Acquisition

The children volunteers played Minecraft, a popular video game where the player controls a character that can roam a large 3D procedurally-generated world. The character is able to explore and find resources to build and craft objects and use tools using virtual blocks within a virtual world. The game engages the player into a creative and immersive experience where they can interact in a shared virtual world with other children playing at the museum. The brain activity and head acceleration of the participating children were recorded using Muse EEG headsets (Interaxon, Toronto, Ontario, Canada). The headset has seven sensors, two out of these seven sensors were positioned at the frontal region (AF7 and AF8), and two at temporal-parietal region (TP9 and TP10) and the remaining three sensors served as electrical reference located at the forehead. The headset has an integrated accelerometer that was used to measure the head acceleration. EEG data for each channel (namely, TP9, AF7, AF8, and TP10) were measured in microvolts with sampling rate of 220Hz while the acceleration data was recorded at 50 Hz. We also recorded the "headband status data", which is a boolean-valued data stream emitted at 10Hz, separately for each EEG channel. This data was used to determine if the headset is placed on the head properly and electrodes are making good contact with the scalp.

A designated area at the Children's Museum of Houston was set up with chairs facing a blank white wall as a setup to acquire data for the (baseline) rest control condition, and an adjacent larger area where 20 desktop computers were arranged

for playing Minecraft. Initially, the children sat in chairs facing a blank white wall and were fitted with the Muse headbands. Then, they were asked to stare at the wall for 1 minute to obtain a baseline recording of their brain activity with their eyes open. Children were asked to avoid body movement. Afterwards, they were led to the desktops where they could play Minecraft for up to 20 minutes while EEG and acceleration data would be recorded. To record the data streams, we set up five headsets connected to one central hub computer using ASUS and Insignia Bluetooth USB adapters. There was a total of four central hub computers that recorded data from 20 headsets. The MuseLab software included in the Muse SDK was used for visualization and saving the data. The associated timestamps were later used for offline data visualization, rejection and segmentation.

Figure 1. Experimental setup at the Children's Museum of Houston. Brain waves were shown to the public as children played Minecraft.

Signal Pre-processing and Spectro-temporal Analysis

Signal Denoising

Figure 2 depicts the data streams and the pre-processing steps followed for signal denoising. We detected issues with the timing and sampling rate of the headsets, which showed irregular sampling frequencies. Moreover, the data came in packets consisting of slightly different number of samples (due to the limitations of Bluetooth technology). Therefore, we estimated the empirical sampling rates for each headset and subject. We computed the estimated sampling rate by taking the difference between the timestamps locked to the EEG samples. We used the interval information to compute the estimated sampling rate by dividing the number of samples by their time stamp interval. The estimated sampling rates shows the mean sampling rate of 219.90 Hz (SD: 1.55 Hz) for EEG and 50 Hz (SD: 0.59 Hz) for accelerometer data. After estimating the empirical sampling rates, both EEG and accelerometer data were resampled to the sampling rate of EEG.

An online notch filter was applied on EEG data while recording it (available as a consumer preset for Muse headbands) to remove the 60 Hz power line noise. We also applied an offline 8th order, zero-phase Butterworth band-pass filter [1-100 Hz] to remove both low and high frequency noise from EEG data. To remove the high-frequency noise from accelerometer data, we used a 3^{rd} order, zero-phase Butterworth low-pass filter with frequency cutoff of 10 Hz after linear detrending. The acceleration data was converted from mg units to m/s^2. Because the children were sitting during the task and we are only interested in the absolute magnitude of acceleration, 9.8 m/s^2 was subtracted from the absolute root mean squared value of the acceleration along all three axes to approximately remove the absolute value of acceleration due to gravity.

Afterwards, the data was inspected, and abnormal or corrupted data samples or channels were rejected to prepare the data for denoising. This step removed all one-second-long epochs that included any electrode pops (tracked by the headband status

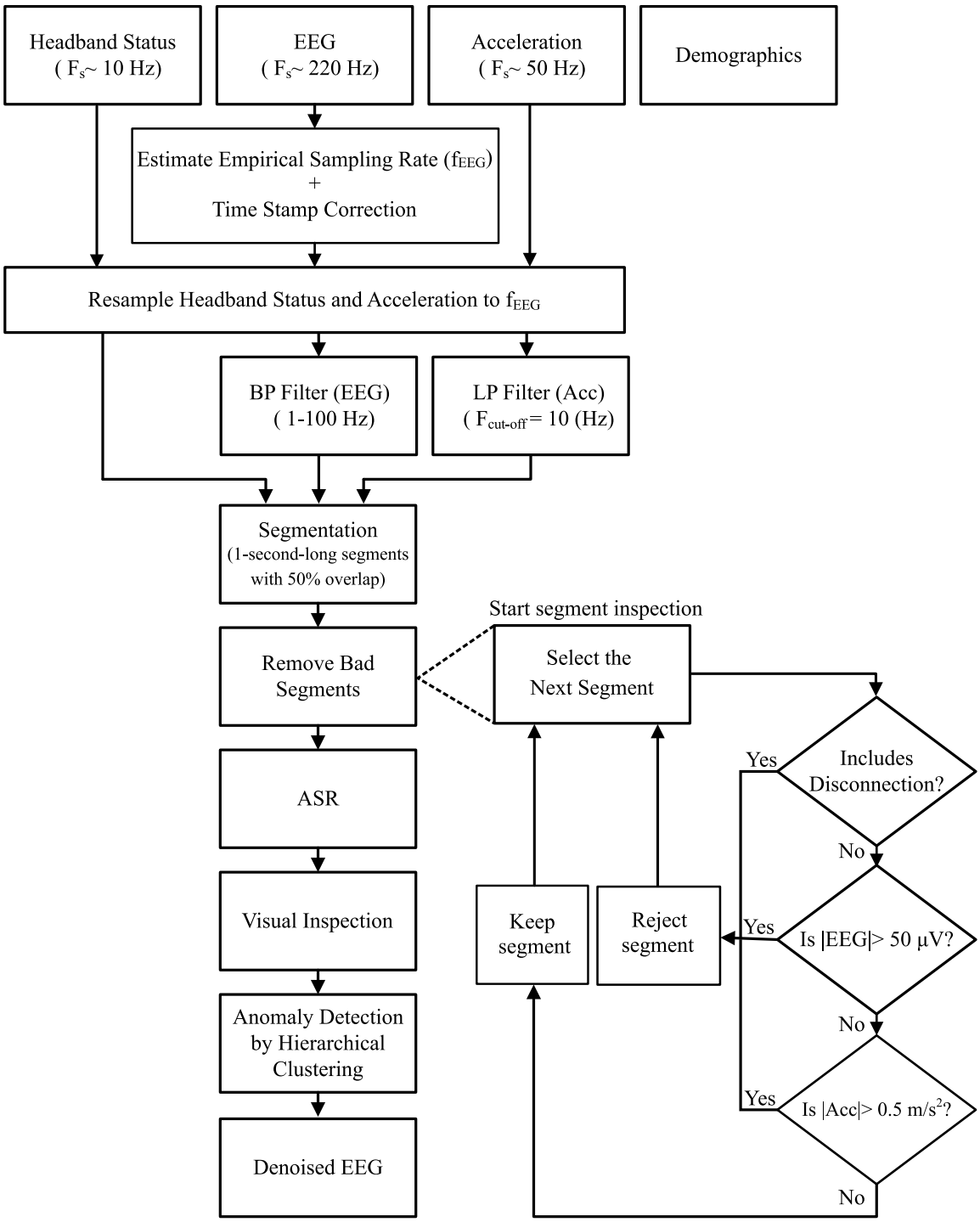

Figure 2. Flowchart illustrating data streams and processing steps for EEG denoising

data), any abrupt change of voltage greater than 50μV or data associated with absolute acceleration values larger than 0.5m/s^2. Next, Artifact Subspace Reconstruction (ASR)[28], which is available as a plug-in through EEGLAB software[29], was used to remove short-time high-amplitude artifacts in the continuous data; from stereotypical (e.g., eye blinks or eye movements) to non-stereotypical (e.g., movement, jaw clench). One minute of on-task EEG data was manually selected as ASR calibration data for each subject, during which the subjects were quite steady (based on accelerometer data). On-task data was used because the clean baseline data was very short (about 30 seconds) for some of the subjects. A cut off threshold of three standard deviations for identification of corrupted subspaces, a window length of 500 milliseconds with 90% overlap between two successive

windows, and no channel rejection were used for ASR. After implementing ASR, signals from all channels and subjects were visually inspected using time, frequency, and time-frequency domain representations to detect and remove parts of data that did not exhibit the common characteristics of EEG signal. The denoising pipeline (removing bad data before ASR, implementing ASR and removing distorted or flattened data after ASR via visual inspection) is illustrated on a 30-second long example of EEG data in the supplementary section (Figure 1 in supplementary section)

Spectral Analysis

The denoised EEG signals were segmented into 1-second windows with 50% overlap. One-sided power spectral density (PSD) of these segments were estimated using the Thomson's multitaper method (pmtm) as implemented in Matlab (Signal Processing Toolbox Version 7.4, the MathWorks, Inc., Natick, Massachusetts, United States). The sampling frequency parameter was kept as 220 and the time-half bandwidth was set to $n_w = 4$, which corresponded to the use of seven discrete prolate spheroidal sequences as data tapers for the multitaper estimation method. This was done for all segments across all channels and subjects. The relative power was computed by expressing the power in each band as a fraction of the total power within 1 -50 Hz frequency range.

Anomaly Detection based on Hierarchical Clustering

As a final stage of pre-processing, hierarchical clustering using Matlab (Statistical and Machine Learning Toolbox version 11.1, the MathWorks, Inc., Natick, Massachusetts, United States), was performed on the 1-second-long segments to detect and reject anomalous segments from both game playing and baseline conditions (see Figure 2). The Pdist function in Matlab was used to compute the dissimilarity/distance between different PSDs. This distance function was used to build the hierarchical cluster tree using the Linkage function in Matlab. Here, an agglomerative bottom up approach was used in which each observation (PSD of the segment) starts in its own cluster, and pairs of clusters are merged as one moves up the hierarchy. The cophenetic correlation coefficient was used to find the best distance metric. This coefficient measures the linear correlation between the cophenetic distances obtained from the tree, and the original distances (or dissimilarities) used to construct the tree. The magnitude of this value should be very close to 1 for a high-quality solution.

Regression Analysis

The mean values of the absolute and relative band powers along with sample entropy[30] was computed for each age groups (6-16 age). A linear regression model $y = ax + b$ was estimated as a function of age(dependent variable y) with each of these features(a), separately. A p-value < 0.05 was considered statistically significant.

Kernel K-means Clustering

Kernel K-means is the nonlinear version of the K-means algorithm that was proposed to detect arbitrary shaped clusters with a proper choice of kernel function[31]. Kernel function is a non-linear transformation that maps the input data to a new high dimensional space (Hilbert space) to increase the separability among data examples[32]. In this study, we used Kernel K-means to partition all patterns that were observed in the PSDs across all subjects. This was done for each channel and for each condition separately. The magnitude of PSDs at 50 integer frequencies (1-50 Hz) were used as features. These spectral features were also normalized prior to clustering to have zero mean and equal standard deviation to make the clustering faster and more accurate. Principal component analysis (PCA) was performed on the PSDs to reduce its dimension. The data was projected on to the first 10 principal components for the frontal channels and to 11 PCs for the temporal channels. These PCs explained for 95% of variance in the data. The kernel clustering was applied on this lower dimensional data. Gaussian (RBF) kernel was found to be the most suitable kernel function for clustering the data in hand as witnessed by the lower values of cost function (computed as the sum of squared distances between single PSDs and the centroid of the clusters). Median of the Euclidean distances among all normalized PSDs was also selected as the standard deviation of the Gaussian function. This value found to be the most appropriate one (for all channels and conditions) as it generates kernel matrices with elements well-distributed in range [0, 1] and also reduces the value of cost function (compared with other proposed metrics).

As proposed by[33], eigenvalues of the kernel matrix provides a means to estimate the number of clusters inherent within the data. This can be done by computing the eigenvalue decomposition of the kernel matrix ($\mathbf{K} = \mathbf{U}\Lambda\mathbf{U}^{\mathbf{T}}$) and subsequently terms $\lambda_i 1_N^T u_i\}^2$ where λ_i is the i^{th} eigenvalue associated to eigenvector u_i and 1_N is an N×1 dimensional vector with elements of value 1/N where N is the total number of samples. The L dominant terms provides an estimation of the possible number of clusters within the data sample. In this study, we sorted these values in descending order and computed the ratio:

$$R = \frac{\sum_{i=1}^{L} \lambda_i \{1_N^T u_i\}^2}{\sum_{i=1}^{N} \lambda_i \{1_N^T u_i\}^2} \tag{1}$$

We selected L (the number of clusters) as the smallest integer value satisfying $R > 0.99$.

Results

Demographics and Data Statistics

Information about age, gender, race and level of expertise in playing Minecraft was collected from children as demographic data and are summarized in Figure 3. The age of participants ranged from 6 to 16 years, with an average age of 8.83 (SD: 2.34). Multiple studies have reported significant developmental changes to occur in the frontal region of the brain during 11-12 years of age and 10-11 years in the parietal regions[13,34–37] . Since the muse system has active channels in the frontal and temporoparietal regions, we assigned the children into two separate groups (young: <=10, older: >=11).

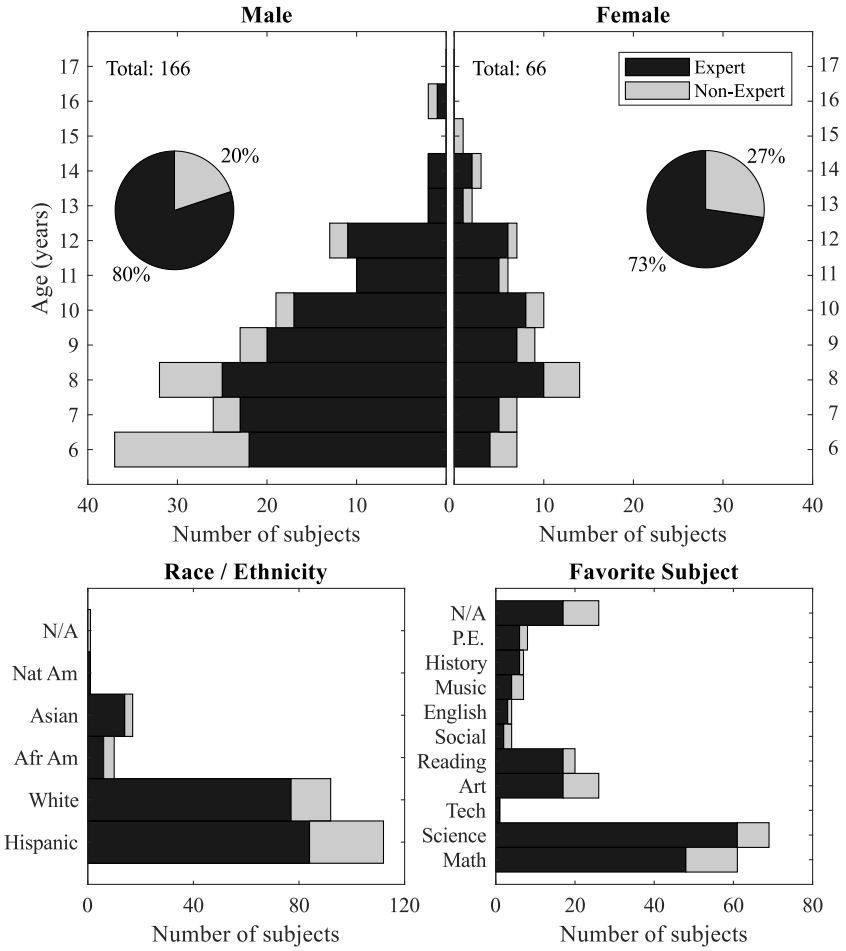

Figure 3. Demographics of participants in the study. Race, age, skill level, gender, Favorite subject are shown for the entire population. Nat Am: Native Americans, Afr Am: African Americans,P.E.: Physical Education, N/A: Not available, Tech: Technology

Data Denoising

Some data recordings were lost due to several factors: 1) EEG headsets had to be recharged often and we were not able to record data from 40 subjects. As a result, MoBI data was only collected from 197 subjects (out of 235 participants). Moreover, from this sample of 197 data sets, 39 datasets had empty data due to data corruption and Bluetooth connectivity issues, leaving 158 (127M/49F) usable data sets. However, some of these datasets did not have long segments of clean data in both baseline and task conditions due to poor placement or fitting of the device on the user's head resulting in poor electrode contact. In addition, baseline data was not possible to record in some participants. Hence the final experimental sample included in the analysis consisted of 88 (67 M, 21 F) children, which had clean EEG segments after the preprocessing stages.

Anomaly Detection (Outliers)

To remove the potential outliers from the data before characterizing the spectral patterns, we used agglomerative hierarchical clustering on the PSDs for outlier detection. After creating the tree of binary clusters, it was pruned to extract the clusters of clean PSDs. An outlier is typically a data point which differs significantly from others. Therefore, instead of limiting the maximum number of clusters, inconsistency coefficients (the relative consistency of each link in a hierarchical cluster tree) were computed and utilized as the criterion to find the appropriate number of clusters. This value compares the height of a link in a cluster hierarchy with the average height of links below it and is capable of identifying the divisions where the similarities between PSDs change abruptly. Here, an empirically chosen threshold of 0.8 of the inconsistency coefficient of the last link was used as the cutoff threshold for all subjects. In building the tree of hierarchical clusters, correlation coefficients were computed for various methods and measures of computing distance between PSDs and cluster of PSDs. Finally, Euclidean distance and unweighted average distance (UPGMA) method by[38]. were selected as the distance metric between PSDs and cluster of PSDs, respectively, as they lead to comparatively higher cophenet correlation coefficients (0.86 ± 0.06 and 0.83±0.04 for baseline and task conditions respectively) for all subjects and channels.

For most of the subjects, hierarchical clustering led to 3 unbalanced clusters, one of which is significantly larger than the other two. For baseline condition, about 80 ± 12, 72 ± 20, 78 ± 15, and 83 ± 7 percent of all segments were clustered in the largest cluster for channel TP9, AF7, AF8, TP10, respectively. These percentages are 89 ± 8, 83 ± 16 and 86 ± 13, and 88 ± 5 for TP9, AF7, AF8, TP10 channels, respectively, during the task (game-playing) condition.

We found that most of the PSDs (between 70 to 90%) were grouped in one cluster for both conditions across all subjects. Considering that the children were involved in playing the video game for most of the recording duration, we assume that the largest cluster for each subject, channel and condition is associated with the desired task while the smaller clusters (representing very few PSDs) might be associated with non-task-related activities (such as children talking) or represent artifacts that were not identified nor removed in the denoising stage (such as large peaks without 1/f power law) of the smaller clusters. With this assumption, the data segments belonging to the largest cluster were selected for further analysis.

Regression analysis with age

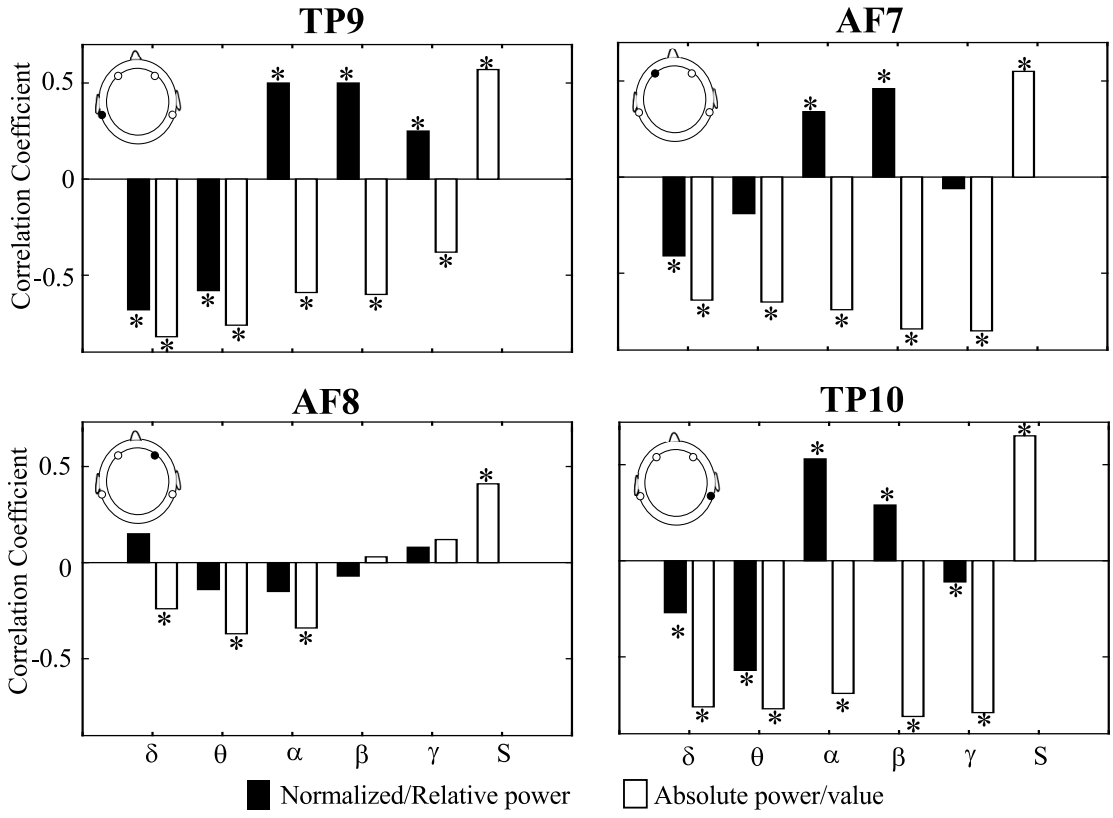

Figure 4. Age-related regression analysis during baseline condition. The correlation coefficient (r) for the linear regression model between the age of the subjects and band-power or sample entropy features. δ: delta power, θ: theta power, α: alpha power, β: beta power, γ: gamma power, S: Sample Entropy, *: indicates significance at $p < 0:05$.

We analyzed the variation of sample entropy, absolute and relative band powers with age during the baseline condition. For both the temporal channels, the absolute power reduced in all frequency bands with age($p < 0.5$; all comparisons). In the frontal channels the absolute power dropped in all bands except for beta and gamma in AF8. The sample entropy increased in all four channels with age($p < 0.5$; all comparisons).

In both temporal channels, the relative band powers in delta and theta band, decreased as a function of age. The alpha and beta power on the other hand increased. The frontal channels showed similar trend except for a few exceptions. Delta power decreased in AF7 channel during baseline. However, the increase in delta power with age, during baseline for AF8 was not significant at $p < 0.05$.

Relative alpha and beta power increased while the gamma power dropped for AF7 channel with age. The r value for each of these features are shown in Figure 4.

Identifying task-relevant spectral patterns using Kernel K-means clustering

Kernel K-means clustering was performed on the PSDs of the 88 children used for analysis, for both baseline and task conditions across the four channels separately. The clustering was performed after performing principal component analysis (PCA) to reduce the dimension of the PSD data. Mean with Standard Error(SE) PSD of segments in each cluster is depicted for each condition and across all four channels, separately. The distribution of skill level (novice vs. expert) and age group ($<= 10$ and > 10 years of age) for each of the clusters are shown in the adjacent multilayered pie charts. Each of the outer rings is weighted such that rings add up to 100% percentage in each subclass. We did not find significant gender differences. The resulting clusters and the cluster distribution are shown in Figures 5 & 6.

During the baseline condition (Figure 5), most PSDs followed the typical inverse power law except for cluster 2 in AF8 which had a peak in beta frequency. In channel AF7, PSDs were grouped into only 2 clusters. Cluster 1, with relatively higher delta power, is found predominantly in younger subjects, whereas cluster 2, with lower delta power, has a larger representation in older children. Similarly, cluster 3 of AF8, characterized by low delta and theta power, was almost entirely found in older subjects while cluster 4 with higher delta and theta power had dominant representation in younger children. Cluster 2, with a peak in beta frequency was found in younger subjects more compared to older subjects. In TP9 channel, cluster 2 had larger representation in younger children compared to older while cluster 3 had the opposite relation. Cluster 2 in TP10 was almost entirely found in younger children.

During the Minecraft-playing task, cluster 1 in AF7, showed a peak in the gamma frequency band and was almost entirely found in older children who are experts at playing Minecraft. Cluster 3 with higher delta and theta power along with a peak at gamma band is found exclusively in younger children. This cluster also has larger representation in experts compared to novices. Cluster 4 with a peak in beta band predominantly appeared in younger children while cluster 5 was almost entirely seen in older children. The clusters had similar representation across classes in regard to skill level. Similarly, cluster 6 had most of its representation in younger children and was equally represented across skill levels.

In the AF8 channel, cluster 1 with relatively lower delta and theta power and a peak at the beta frequency band had a larger representation in older children. Compared to experts, cluster 1 was represented more in novices. Cluster 2, which also had a higher beta activation, was found only in young children. Cluster 4 with a peak in beta band was almost entirely found in experts. Cluster 4 was represented more in younger subjects. Cluster 2 in both TP9 and TP10, with a peak in lower beta band, had very little representation in older children.

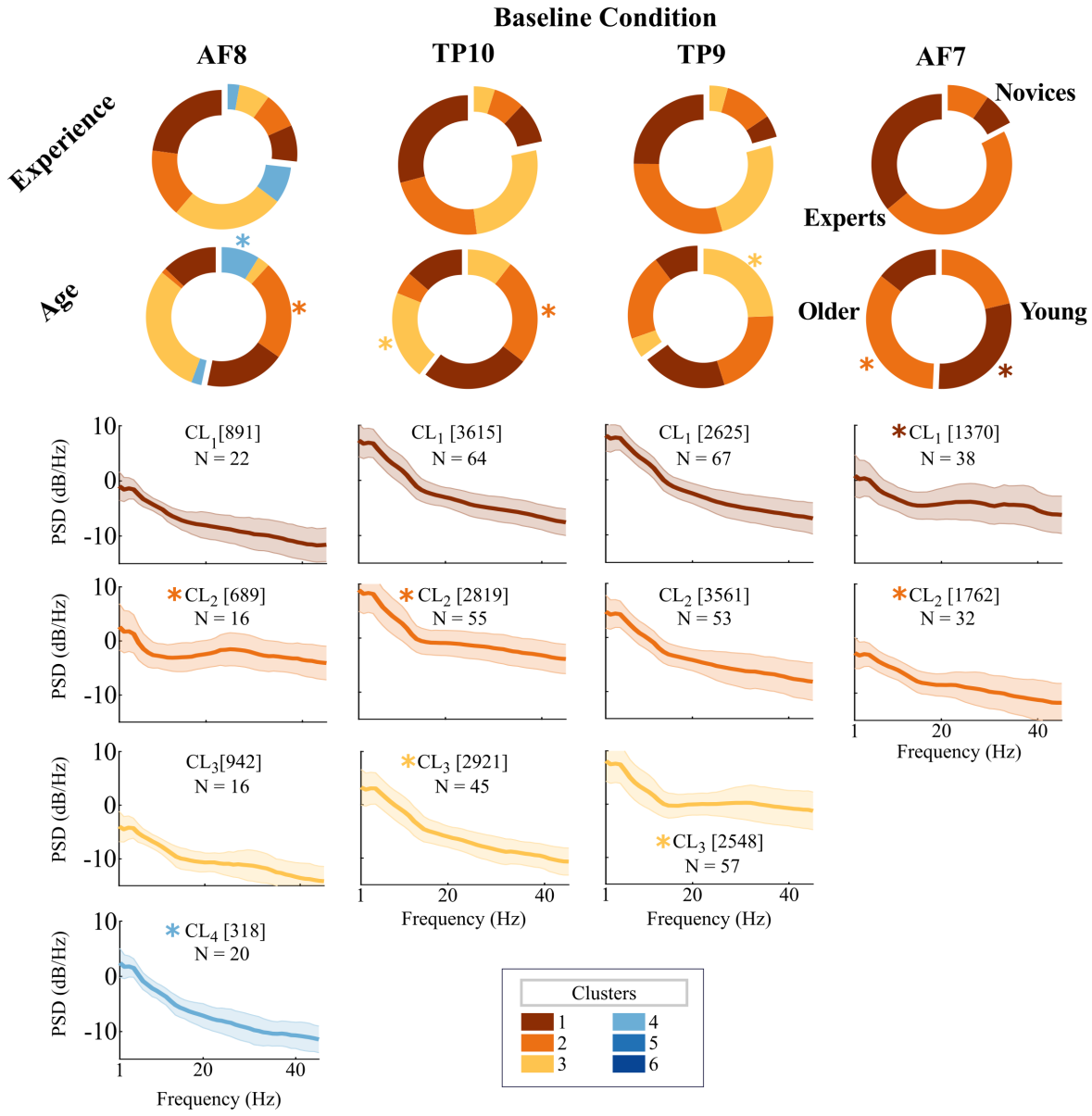

Figure 5. PSD clustering during baseline condition.Skill and age dependencies of power spectral density (PSD) patterns for the baseline conditions. Average PSD (with SE) shown for clusters resulted from Kernel K-means clustering of the PSD segments. Multilayer pie charts show the distribution (in %) of different skill levels and age in each of those clusters.

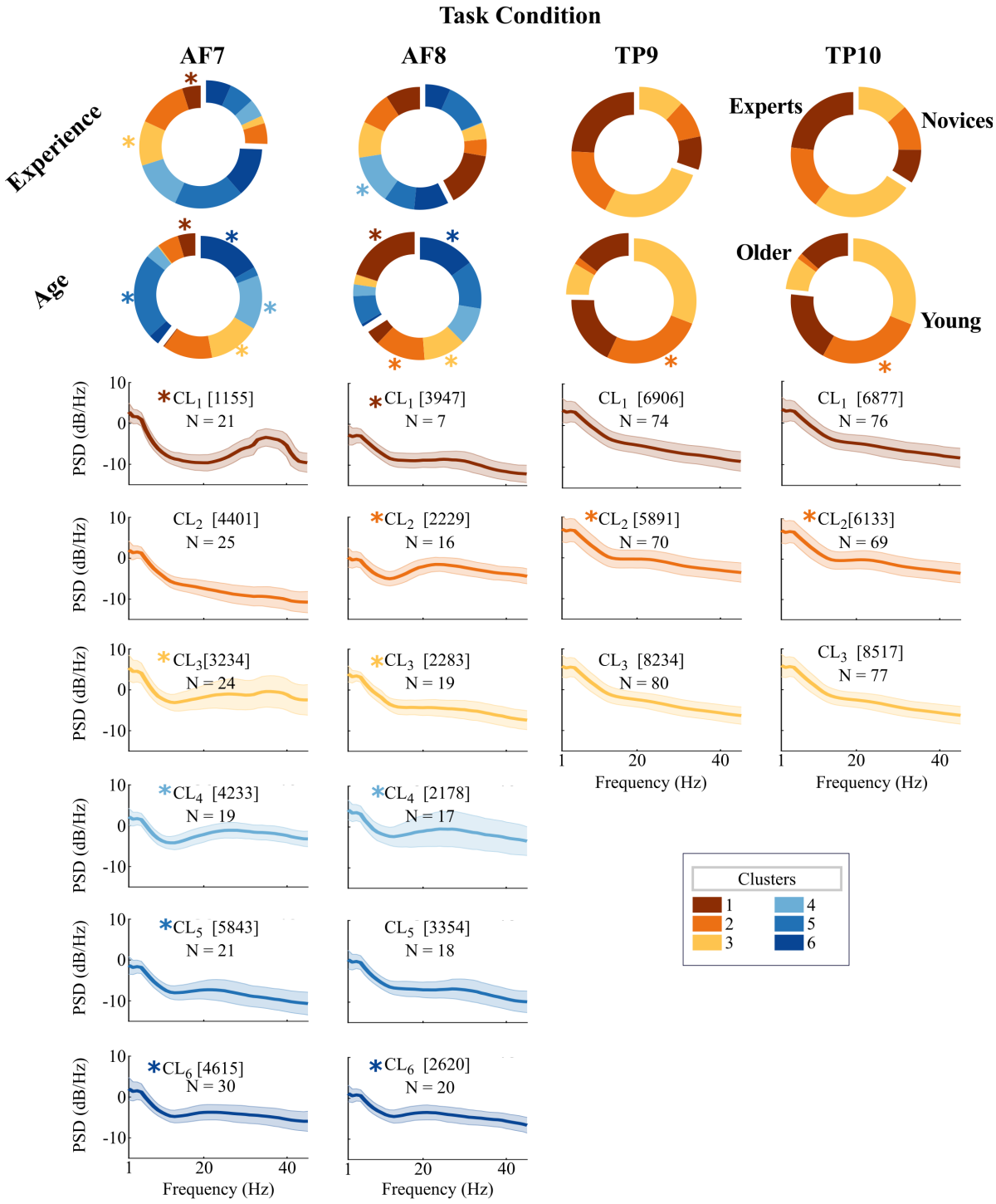

Figure 6. PSD clustering during minecraft playing condition. Skill and age dependencies of PSD patterns during the task condition. Average PSD (with SE) shown for clusters resulted from Kernel K-means clustering of the PSD segments. Multilayer Pie charts show the distribution (in %) of different skill levels and age in each of those clusters.

Discussion

This study demonstrates the feasibility of recording and quantifying EEG patterns among a diverse population of 88 children as they played the Minecraft video game in a natural social environment at the Children's Museum of Houston. This study also validated a novel methodology to identify patterns of electrocortical activity recorded with scalp EEG in an unsupervised fashion. The main findings were: a) Characterized effects of age, gender and skill level on EEG spectral patterns during video game play; b) Observed different sets of PSDs that were predominantly represented in subgroups of children as a function of age, and/or skill level; c) Identified effects of aging on frequency and complexity measures of EEG in a more naturally engaging environment d) Explored the usability of portable EEG in a natural setting. We now discuss the above findings in the context of prior studies and recent neuroscience data.

Overall Data Yield

We had 233 children voluntarily participate in the experiment, but only 88 of the participants produced usable good quality sensor data for further analysis. This represents a yield of only 38% of the total datasets, which is modest. . This was due to several factors: 1) the EEG headsets were not specifically designed for the smaller and varying head shapes of children, which resulted in a poor fit in some children; 2) we did not have enough EEG headsets to allow for replacement during battery charging thus preventing data collection; 3) excessive body/head motion and non-compliant children resulted in low quality data in some cases. We recommend that future experiments should use EEG headsets specifically designed for the pediatric population and have spare EEG headsets available for swapping during recharging.

Spectral power and age

Studies have reported the reduction in EEG band power with age. Reduction in slow wave activity was reported to be accompanied with reduction in gray matter across age[39]. Developmental studies have reported reduced EEG power in all bands as a function of age in children[40–44]. Tierney et.al[5] observed the gamma power to drop with age. These findings are consistent with our results. Other studies have analyzed the variation of relative band power with age and have found the relative power to decrease in delta and theta band while increasing in the alpha and beta band[40–45]. Our results are also consistent with prior findings, except for channel AF8.

In regard to sample entropy, it has been reported that it monotonically increases from early to late childhood[46,47]. Empirical studies suggest that sample entropy, which measures the irregularity in brain signal, is expected to increase with age[48]. Our data supports this notion as we observed an increase in sample entropy with age. Our results extend prior findings to data acquired in freely behaving children in a natural environment.

Distribution of spectral patterns of brain activity during the baseline condition

The kernel k-means clustering analysis showed age dependencies during the baseline condition: left prefrontal activity (AF7) generated separated PSD clusters (e.g., CL_1, CL_2) that were associated mainly with younger or older participants. Similarly, right prefrontal activity (AF8), characterized by the lowest delta power among all the clusters, was almost entirely represented in the older subjects, whereas some patterns (CL_4), with higher delta and theta band power, were observed mainly in younger subjects. This is in accordance with the previous literature on the developmental changes on EEG as discussed in the regression analysis. Most PSD patterns of older children followed the inverse frequency power law while many of the PSD patterns of younger subjects had peaks in beta frequency band during baseline. This might be because the younger children are anticipating more and might be excited about the game play even during baseline. Different studies have reported that pre-frontal beta activation could be associated with anticipation[49] .

Distribution of spectral patterns of brain activity during the videogame condition

During the videogame condition, left prefrontal area (AF7) showed a peak at gamma band of older expert subjects (CL_1). Another cluster of PSDs (CL_3) showed had a peak in gamma frequency of skilled children with Minecraft experience, whereas cluster CL_1 was observed in younger children more. This might indicate that higher gamma power might be associated with skill level. In this regards, higher gamma activity has reported to been associated with cognitive functions such as attention, object recognition, learning and memory[5,50–54]. Minecraft involves, planning, observation and object representation all of which could elicit similar response. The expert players might be more attentive and involved in the game which might be the reason for the representation to be present mainly in experts. It might also correspond to instances wherein the subjects were highly involved in the game play.

Another cluster found in the left prefrontal channel was characterized with a small peak in the beta frequency band and was almost entirely found in older children (CL_5). This large cluster had equal representation among children with different skill levels. This might suggest that it could be characteristic of the age group. The assumption is plausible, as that cluster has the lowest delta and theta power among other clusters while having a peak at beta frequency which fits into the characteristics

described earlier in the regression analysis for older subjects. Interestingly, another cluster (CL_6) with relatively higher delta and theta power was almost entirely comprised of younger children. Increases in theta rhythm has been previously reported with increases in mental load/ attention during video game play[22,23,55]. Also, beta power was found to increase in occipital, parietal, frontal and motor region while playing video game[24]. Beta activity has also been associated with alert attentiveness in different studies[25].

The right prefrontal cortex (AF8) had PSD clusters with peak in the beta frequencies that were predominantly see in older (CL_1) or younger (CL_2) children, perhaps attentiveness to the task. The clustering makes sense as cluster 1 has lower power in delta and theta bands compared to cluster 2 characteristic of the age groups. Cluster 4, which has a relatively higher overall power and a peak in the beta band, was found almost entirely in skilled players.

During the video-playing task condition, both temporal channels (TP9 and TP10) had PSDs grouped into a cluster (cluster 2) with a peak in the beta band; found primarily in younger subjects. These PSDs were found in 85% of the subjects under 10 years of age. This suggest it to be a characteristic pattern expected to be observed in younger subjects during video game play. Cluster 3 in both temporal channels had contribution from almost 91% of total participants, suggesting this pattern to be common across our subject population. It did not show a dominance towards any particular age category or skill level. Finally, a lower number of clusters in temporal electrodes might indicate lower variability in that area associated with video game play in comparison to frontal electrodes. This is consistent with a role of prefrontal cortex in higher-order function such as decision making during gameplay.

In summary, we identified spectral patterns of brain activity during baseline and Minecraft playing; some these patterns showed dependencies of age and skill levels, but not gender. We also confirmed that the observations of age related changes in baseline EEG features previously reported in laboratory settings were generally consistent in more naturally engaging environment as well. We proposed the application of an unsupervised method of pattern recognition in EEG studies and uncovered group relevant spectral patterns. Overall, the current study contributes to a better understanding of the population distribution of EEG-based biometrics (e.g., spectral content) in children, and their variation with respect to age and skill level in a more natural and engaging environment. The MoBI data analyzed in this study is available to the scientific community in IEEE Dataport(DOI :10.21227/H23W88).

References

1. Kovacevic, N., Ritter, P., Tays, W., Moreno, S. & McIntosh, A. R. 'my virtual dream': Collective neurofeedback in an immersive art environment. *PloS one* **10**, e0130129 (2015).
2. Kontson, K. L. *et al.* Your brain on art: emergent cortical dynamics during aesthetic experiences. *Front. human neuroscience* **9** (2015).
3. Cruz-Garza, J. G. *et al.* Deployment of mobile eeg technology in an art museum setting: Evaluation of signal quality and usability. *Front. Hum. Neurosci.* **11**, 527 (2017).
4. Benasich, A. A., Gou, Z., Choudhury, N. & Harris, K. D. Early cognitive and language skills are linked to resting frontal gamma power across the first 3 years. *Behav. brain research* **195**, 215–222 (2008).
5. Tierney, A., Strait, D. L., O'Connell, S. & Kraus, N. Developmental changes in resting gamma power from age three to adulthood. *Clin. neurophysiology: official journal Int. Fed. Clin. Neurophysiol.* **124**, 1040 (2013).
6. Vlahou, E. L., Thurm, F., Kolassa, I.-T. & Schlee, W. Resting-state slow wave power, healthy aging and cognitive performance. *Sci. reports* **4** (2014).
7. Zappasodi, F., Marzetti, L., Olejarczyk, E., Tecchio, F. & Pizzella, V. Age-related changes in electroencephalographic signal complexity. *PloS one* **10**, e0141995 (2015).
8. Perlman, J. M. Cognitive and behavioral deficits in premature graduates of intensive care. *Clin. perinatology* **29**, 779–797 (2002).
9. on Children with Disabilities, C. *et al.* The pediatrician's role in the diagnosis and management of autistic spectrum disorder in children. *Pediatr.* **107**, 1221–1226 (2001).
10. Chabot, R. J. & Serfontein, G. Quantitative electroencephalographic profiles of children with attention deficit disorder. *Biol. psychiatry* **40**, 951–963 (1996).
11. Kamida, A. *et al.* Eeg power spectrum analysis in children with adhd. *Yonago acta medica* **59**, 169 (2016).
12. Chu, Y.-J., Chang, C.-F., Shieh, J.-S. & Lee, W.-T. The potential application of multiscale entropy analysis of electroencephalography in children with neurological and neuropsychiatric disorders. *Entropy* **19**, 428 (2017).

13. Segalowitz, S. J., Santesso, D. L. & Jetha, M. K. Electrophysiological changes during adolescence: a review. *Brain cognition* **72**, 86–100 (2010).

14. Stroganova, T. A., Orekhova, E. V. & Posikera, I. N. Eeg alpha rhythm in infants. *Clin. Neurophysiol.* **110**, 997–1012 (1999).

15. Marshall, P. J., Bar-Haim, Y. & Fox, N. A. Development of the eeg from 5 months to 4 years of age. *Clin. Neurophysiol.* **113**, 1199–1208 (2002).

16. Soroko, S., Shemyakina, N., Nagornova, Z. V. & Bekshaev, S. Longitudinal study of eeg frequency maturation and power changes in children on the russian north. *Int. J. Dev. Neurosci.* **38**, 127–137 (2014).

17. Marcuse, L. *et al.* Quantitative analysis of the eeg posterior-dominant rhythm in healthy adolescents. *Clin. neurophysiology* **119**, 1778–1781 (2008).

18. Gramann, K. *et al.* Cognition in action: imaging brain/body dynamics in mobile humans. *Rev. Neurosci.* **22**, 593–608 (2011).

19. Entertainment-Software-Association. Essential facts about the computer and video game industry (2017). URL http://www.theesa.com/article/2017-essential-facts-computer-video-game-industry.

20. Lenhart, A. *et al.* Teens, video games, and civics: Teens' gaming experiences are diverse and include significant social interaction and civic engagement. *Pew internet & Am. life project* (2008).

21. Mathewson, K. E. *et al.* Different slopes for different folks: Alpha and delta eeg power predict subsequent video game learning rate and improvements in cognitive control tasks. *Psychophysiol.* **49**, 1558–1570 (2012).

22. He, E. J., Yuan, H., Yang, L., Sheikholeslami, C. & He, B. Eeg spatio-spectral mapping during video game play. In *Information Technology and Applications in Biomedicine, 2008. ITAB 2008. International Conference on*, 346–348 (IEEE, 2008).

23. Pellouchoud, E., Smith, M. E., McEvoy, L. & Gevins, A. Mental effort-related eeg modulation during video-game play: Comparison between juvenile subjects with epilepsy and normal control subjects. *Epilepsia* **40**, 38–43 (1999).

24. Malik, A. S., Osman, D. A., Pauzi, A. A. & Khairuddin, R. H. R. Investigating brain activation with respect to playing video games on large screens. In *Intelligent and Advanced Systems (ICIAS), 2012 4th International Conference on*, vol. 1, 86–90 (IEEE, 2012).

25. Salminen, M. & Ravaja, N. Oscillatory brain responses evoked by video game events: The case of super monkey ball 2. *CyberPsychology & Behav.* **10**, 330–338 (2007).

26. Skoric, M. M., Teo, L. L. C. & Neo, R. L. Children and video games: addiction, engagement, and scholastic achievement. *Cyberpsychology & behavior* **12**, 567–572 (2009).

27. Attfield, S., Kazai, G., Lalmas, M. & Piwowarski, B. Towards a science of user engagement (position paper). In *WSDM workshop on user modelling for Web applications*, 9–12 (2011).

28. Mullen, T. *et al.* Real-time modeling and 3d visualization of source dynamics and connectivity using wearable eeg. In *Engineering in Medicine and Biology Society (EMBC), 2013 35th Annual International Conference of the IEEE*, 2184–2187 (IEEE, 2013).

29. Delorme, A. & Makeig, S. Eeglab: an open source toolbox for analysis of single-trial eeg dynamics including independent component analysis. *J. neuroscience methods* **134**, 9–21 (2004).

30. Richman, J. S. & Moorman, J. R. Physiological time-series analysis using approximate entropy and sample entropy. *Am. J. Physiol. Circ. Physiol.* **278**, H2039–H2049 (2000).

31. Jain, A. K. Data clustering: 50 years beyond k-means. *Pattern recognition letters* **31**, 651–666 (2010).

32. Zhang, R. & Rudnicky, A. I. A large scale clustering scheme for kernel k-means. In *Pattern Recognition, 2002. Proceedings. 16th International Conference on*, vol. 4, 289–292 (IEEE, 2002).

33. Girolami, M. Mercer kernel-based clustering in feature space. *IEEE Transactions on Neural Networks* **13**, 780–784 (2002).

34. Passler, M. A., Isaac, W. & Hynd, G. W. Neuropsychological development of behavior attributed to frontal lobe functioning in children. *Dev. Neuropsychol.* **1**, 349–370 (1985).

35. Giedd, J. N. *et al.* Brain development during childhood and adolescence: a longitudinal mri study. *Nat. neuroscience* **2**, 861–863 (1999).

36. Blakemore, S.-J. & Choudhury, S. Development of the adolescent brain: implications for executive function and social cognition. *J. child psychology psychiatry* **47**, 296–312 (2006).

37. Lebel, C., Walker, L., Leemans, A., Phillips, L. & Beaulieu, C. Microstructural maturation of the human brain from childhood to adulthood. *Neuroimage* **40**, 1044–1055 (2008).

38. Sokal, R. R. A statistical method for evaluating systematic relationship. *Univ. Kansas science bulletin* **28**, 1409–1438 (1958).

39. Whitford, T. J. *et al.* Brain maturation in adolescence: concurrent changes in neuroanatomy and neurophysiology. *Hum. brain mapping* **28**, 228–237 (2007).

40. Gasser, T., Verleger, R., Bächer, P. & Sroka, L. Development of the eeg of school-age children and adolescents. i. analysis of band power. *Electroencephalogr. clinical neurophysiology* **69**, 91–99 (1988).

41. Clarke, A. R., Barry, R. J., McCarthy, R. & Selikowitz, M. Age and sex effects in the eeg: development of the normal child. *Clin. neurophysiology* **112**, 806–814 (2001).

42. Gmehlin, D. *et al.* Individual analysis of eeg background-activity within school age: impact of age and sex within a longitudinal data set. *Int. J. Dev. Neurosci.* **29**, 163–170 (2011).

43. Barriga-Paulino, C. I., Flores, A. B. & Gómez, C. M. Developmental changes in the eeg rhythms of children and young adults. *J. Psychophysiol.* (2011).

44. Miskovic, V. *et al.* Developmental changes in spontaneous electrocortical activity and network organization from early to late childhood. *Neuroimage* **118**, 237–247 (2015).

45. Niemarkt, H. J. *et al.* Maturational changes in automated eeg spectral power analysis in preterm infants. *Pediatr. research* **70**, 529–534 (2011).

46. De Wel, O. *et al.* Complexity analysis of neonatal eeg using multiscale entropy: Applications in brain maturation and sleep stage classification. *Entropy* **19**, 516 (2017).

47. Miskovic, V., Owens, M., Kuntzelman, K. & Gibb, B. E. Charting moment-to-moment brain signal variability from early to late childhood. *Cortex* **83**, 51–61 (2016).

48. McIntosh, A. R. *et al.* The development of a noisy brain. *Arch. italiennes de biologie* **148**, 323–337 (2010).

49. Altamura, M. *et al.* Prefrontal cortex modulation during anticipation of working memory demands as revealed by magnetoencephalography. *J. Biomed. Imaging* **2010**, 12 (2010).

50. Tiitinen, H. *et al.* Selective attention enhances the auditory 40-hz transient response in humans. *Nat.* **364**, 59–60 (1993).

51. Keil, A., Müller, M. M., Ray, W. J., Gruber, T. & Elbert, T. Human gamma band activity and perception of a gestalt. *J. Neurosci.* **19**, 7152–7161 (1999).

52. Başar, E., Başar-Eroğlu, C., Karakaş, S. & Schürmann, M. Brain oscillations in perception and memory. *Int. journal psychophysiology* **35**, 95–124 (2000).

53. Kaiser, J. & Lutzenberger, W. Induced gamma-band activity and human brain function. *The Neurosci.* **9**, 475–484 (2003).

54. Kaiser, J. & Lutzenberger, W. Human gamma-band activity: a window to cognitive processing. *Neuroreport* **16**, 207–211 (2005).

55. Yamada, F. Frontal midline theta rhythm and eyeblinking activity during a vdt task and a video game: useful tools for psychophysiology in ergonomics. *Ergonomics* **41**, 678–688 (1998).

References

1. Kovacevic, N., Ritter, P., Tays, W., Moreno, S. & McIntosh, A. R. 'my virtual dream': Collective neurofeedback in an immersive art environment. *PloS one* **10**, e0130129 (2015).

2. Kontson, K. L. *et al.* Your brain on art: emergent cortical dynamics during aesthetic experiences. *Front. human neuroscience* **9** (2015).

3. Cruz-Garza, J. G. *et al.* Deployment of mobile eeg technology in an art museum setting: Evaluation of signal quality and usability. *Front. Hum. Neurosci.* **11**, 527 (2017).

4. Benasich, A. A., Gou, Z., Choudhury, N. & Harris, K. D. Early cognitive and language skills are linked to resting frontal gamma power across the first 3 years. *Behav. brain research* **195**, 215–222 (2008).

5. Tierney, A., Strait, D. L., O'Connell, S. & Kraus, N. Developmental changes in resting gamma power from age three to adulthood. *Clin. neurophysiology: official journal Int. Fed. Clin. Neurophysiol.* **124**, 1040 (2013).

6. Vlahou, E. L., Thurm, F., Kolassa, I.-T. & Schlee, W. Resting-state slow wave power, healthy aging and cognitive performance. *Sci. reports* **4** (2014).

7. Zappasodi, F., Marzetti, L., Olejarczyk, E., Tecchio, F. & Pizzella, V. Age-related changes in electroencephalographic signal complexity. *PloS one* **10**, e0141995 (2015).

8. Perlman, J. M. Cognitive and behavioral deficits in premature graduates of intensive care. *Clin. perinatology* **29**, 779–797 (2002).

9. on Children with Disabilities, C. *et al.* The pediatrician's role in the diagnosis and management of autistic spectrum disorder in children. *Pediatr.* **107**, 1221–1226 (2001).

10. Chabot, R. J. & Serfontein, G. Quantitative electroencephalographic profiles of children with attention deficit disorder. *Biol. psychiatry* **40**, 951–963 (1996).

11. Kamida, A. *et al.* Eeg power spectrum analysis in children with adhd. *Yonago acta medica* **59**, 169 (2016).

12. Chu, Y.-J., Chang, C.-F., Shieh, J.-S. & Lee, W.-T. The potential application of multiscale entropy analysis of electroencephalography in children with neurological and neuropsychiatric disorders. *Entropy* **19**, 428 (2017).

13. Segalowitz, S. J., Santesso, D. L. & Jetha, M. K. Electrophysiological changes during adolescence: a review. *Brain cognition* **72**, 86–100 (2010).

14. Stroganova, T. A., Orekhova, E. V. & Posikera, I. N. Eeg alpha rhythm in infants. *Clin. Neurophysiol.* **110**, 997–1012 (1999).

15. Marshall, P. J., Bar-Haim, Y. & Fox, N. A. Development of the eeg from 5 months to 4 years of age. *Clin. Neurophysiol.* **113**, 1199–1208 (2002).

16. Soroko, S., Shemyakina, N., Nagornova, Z. V. & Bekshaev, S. Longitudinal study of eeg frequency maturation and power changes in children on the russian north. *Int. J. Dev. Neurosci.* **38**, 127–137 (2014).

17. Marcuse, L. *et al.* Quantitative analysis of the eeg posterior-dominant rhythm in healthy adolescents. *Clin. neurophysiology* **119**, 1778–1781 (2008).

18. Gramann, K. *et al.* Cognition in action: imaging brain/body dynamics in mobile humans. *Rev. Neurosci.* **22**, 593–608 (2011).

19. Entertainment-Software-Association. Essential facts about the computer and video game industry (2017). URL http://www.theesa.com/article/2017-essential-facts-computer-video-game-industry.

20. Lenhart, A. *et al.* Teens, video games, and civics: Teens' gaming experiences are diverse and include significant social interaction and civic engagement. *Pew internet & Am. life project* (2008).

21. Mathewson, K. E. *et al.* Different slopes for different folks: Alpha and delta eeg power predict subsequent video game learning rate and improvements in cognitive control tasks. *Psychophysiol.* **49**, 1558–1570 (2012).

22. He, E. J., Yuan, H., Yang, L., Sheikholeslami, C. & He, B. Eeg spatio-spectral mapping during video game play. In *Information Technology and Applications in Biomedicine, 2008. ITAB 2008. International Conference on*, 346–348 (IEEE, 2008).

23. Pellouchoud, E., Smith, M. E., McEvoy, L. & Gevins, A. Mental effort-related eeg modulation during video-game play: Comparison between juvenile subjects with epilepsy and normal control subjects. *Epilepsia* **40**, 38–43 (1999).

24. Malik, A. S., Osman, D. A., Pauzi, A. A. & Khairuddin, R. H. R. Investigating brain activation with respect to playing video games on large screens. In *Intelligent and Advanced Systems (ICIAS), 2012 4th International Conference on*, vol. 1, 86–90 (IEEE, 2012).

25. Salminen, M. & Ravaja, N. Oscillatory brain responses evoked by video game events: The case of super monkey ball 2. *CyberPsychology & Behav.* **10**, 330–338 (2007).

26. Skoric, M. M., Teo, L. L. C. & Neo, R. L. Children and video games: addiction, engagement, and scholastic achievement. *Cyberpsychology & behavior* **12**, 567–572 (2009).

27. Attfield, S., Kazai, G., Lalmas, M. & Piwowarski, B. Towards a science of user engagement (position paper). In *WSDM workshop on user modelling for Web applications*, 9–12 (2011).

28. Mullen, T. *et al.* Real-time modeling and 3d visualization of source dynamics and connectivity using wearable eeg. In *Engineering in Medicine and Biology Society (EMBC), 2013 35th Annual International Conference of the IEEE*, 2184–2187 (IEEE, 2013).

29. Delorme, A. & Makeig, S. Eeglab: an open source toolbox for analysis of single-trial eeg dynamics including independent component analysis. *J. neuroscience methods* **134**, 9–21 (2004).

30. Richman, J. S. & Moorman, J. R. Physiological time-series analysis using approximate entropy and sample entropy. *Am. J. Physiol. Circ. Physiol.* **278**, H2039–H2049 (2000).

31. Jain, A. K. Data clustering: 50 years beyond k-means. *Pattern recognition letters* **31**, 651–666 (2010).

32. Zhang, R. & Rudnicky, A. I. A large scale clustering scheme for kernel k-means. In *Pattern Recognition, 2002. Proceedings. 16th International Conference on*, vol. 4, 289–292 (IEEE, 2002).

33. Girolami, M. Mercer kernel-based clustering in feature space. *IEEE Transactions on Neural Networks* **13**, 780–784 (2002).

34. Passler, M. A., Isaac, W. & Hynd, G. W. Neuropsychological development of behavior attributed to frontal lobe functioning in children. *Dev. Neuropsychol.* **1**, 349–370 (1985).

35. Giedd, J. N. *et al.* Brain development during childhood and adolescence: a longitudinal mri study. *Nat. neuroscience* **2**, 861–863 (1999).

36. Blakemore, S.-J. & Choudhury, S. Development of the adolescent brain: implications for executive function and social cognition. *J. child psychology psychiatry* **47**, 296–312 (2006).

37. Lebel, C., Walker, L., Leemans, A., Phillips, L. & Beaulieu, C. Microstructural maturation of the human brain from childhood to adulthood. *Neuroimage* **40**, 1044–1055 (2008).

38. Sokal, R. R. A statistical method for evaluating systematic relationship. *Univ. Kansas science bulletin* **28**, 1409–1438 (1958).

39. Whitford, T. J. *et al.* Brain maturation in adolescence: concurrent changes in neuroanatomy and neurophysiology. *Hum. brain mapping* **28**, 228–237 (2007).

40. Gasser, T., Verleger, R., Bächer, P. & Sroka, L. Development of the eeg of school-age children and adolescents. i. analysis of band power. *Electroencephalogr. clinical neurophysiology* **69**, 91–99 (1988).

41. Clarke, A. R., Barry, R. J., McCarthy, R. & Selikowitz, M. Age and sex effects in the eeg: development of the normal child. *Clin. neurophysiology* **112**, 806–814 (2001).

42. Gmehlin, D. *et al.* Individual analysis of eeg background-activity within school age: impact of age and sex within a longitudinal data set. *Int. J. Dev. Neurosci.* **29**, 163–170 (2011).

43. Barriga-Paulino, C. I., Flores, A. B. & Gómez, C. M. Developmental changes in the eeg rhythms of children and young adults. *J. Psychophysiol.* (2011).

44. Miskovic, V. *et al.* Developmental changes in spontaneous electrocortical activity and network organization from early to late childhood. *Neuroimage* **118**, 237–247 (2015).

45. Niemarkt, H. J. *et al.* Maturational changes in automated eeg spectral power analysis in preterm infants. *Pediatr. research* **70**, 529–534 (2011).

46. De Wel, O. *et al.* Complexity analysis of neonatal eeg using multiscale entropy: Applications in brain maturation and sleep stage classification. *Entropy* **19**, 516 (2017).

47. Miskovic, V., Owens, M., Kuntzelman, K. & Gibb, B. E. Charting moment-to-moment brain signal variability from early to late childhood. *Cortex* **83**, 51–61 (2016).

48. McIntosh, A. R. *et al.* The development of a noisy brain. *Arch. italiennes de biologie* **148**, 323–337 (2010).

49. Altamura, M. *et al.* Prefrontal cortex modulation during anticipation of working memory demands as revealed by magnetoencephalography. *J. Biomed. Imaging* **2010**, 12 (2010).

50. Tiitinen, H. *et al.* Selective attention enhances the auditory 40-hz transient response in humans. *Nat.* **364**, 59–60 (1993).

51. Keil, A., Müller, M. M., Ray, W. J., Gruber, T. & Elbert, T. Human gamma band activity and perception of a gestalt. *J. Neurosci.* **19**, 7152–7161 (1999).

52. Başar, E., Başar-Eroğlu, C., Karakaş, S. & Schürmann, M. Brain oscillations in perception and memory. *Int. journal psychophysiology* **35**, 95–124 (2000).

53. Kaiser, J. & Lutzenberger, W. Induced gamma-band activity and human brain function. *The Neurosci.* **9**, 475–484 (2003).

54. Kaiser, J. & Lutzenberger, W. Human gamma-band activity: a window to cognitive processing. *Neuroreport* **16**, 207–211 (2005).

55. Yamada, F. Frontal midline theta rhythm and eyeblinking activity during a vdt task and a video game: useful tools for psychophysiology in ergonomics. *Ergonomics* **41**, 678–688 (1998).

Acknowledgements

This research was supported by a cross-cutting seed grant from the Cullen College of Engineering at the University of Houston and by National Science Foundation Award BCS 1533691. We also acknowledge the logistical support of all members of the Noninvasive Brain-Machine Interface Systems Laboratory who assisted with the data collection at the Children's Museum of Houston. This work could not have been done without the support of Julia Banda, Gretchen Schmaltz, and Neelam Damani, Director of Gallery Education at the Children's Museum of Houston.

Author contributions statement

JLC-V conceptualized and supervised the study, was responsible for methodology and acquisition of financial support for the project, and reviewed and edited the manuscript; AM, JGC-G, AP, and AK conducted the experiment at CMH; AM, ASR and SE were responsible for the software and performed the formal analyses under supervision from JLC-V and were involved in data visualization; AM and ASR wrote the first draft; all authors reviewed, edited and provided final approval of the manuscript.

Competing financial interests

The authors declare that the research was conducted in the absence of any commercial or financial relationships that could be construed as a potential conflict of interest.